N = impeller speed
N_i = initial impeller speed for given run
P = fraction of feed stream which undergoes plug flow
PMRTD = perfect mixing residence time distribution
Q = impeller discharge rate or impeller pumping capacity
R = gas constant
R.T.D. = residence time distribution
T = temperature
$\overline{T}$ = average temperature
T_i = inlet reactant temperature
T_o = reactor outlet temperature
t = time
V_T = volume of stirred tank
$\delta(t=0)$ = Dirac delta function
ρ = density
τ = mean holdup time in vessel
$\tau_{1/2}$ = reaction half time
Φ = defined in Table 1

LITERATURE CITED

1. Keairns, D. L., Ph.D. dissertation, Carnegie Inst. Tech., Pittsburgh, Pa. (1967).
2. LaRosa, P. and F. S. Manning, *Can. J. Chem. Eng.*, **42**, 65 (1964).
3. Manning, F. S., D. Wolf, and D. L. Keairns, *AIChE J.*, **11**, 723 (1965).
4. Ng, D. Y. C. and D. W. T. Rippm, Proc. Third European Symposium Chem. Reaction Eng., Amsterdam (Sept., 1964).
5. Spencer, J. L., Ph.D. dissertation, Univ. Pennsylvania (1961).
6. Spencer, J. L., and W. C. Cohen, *Chem. Eng. Progr.*, **58**, (12), 40 (1962).
7. Wolf, D. and F. S. Manning, *Can. J. Chem. Eng.*, **44**, 137 (1966).
8. Worrell, G. R., Ph.D. dissertation, Univ. Pennsylvania (1963).
9. Wu, D. T., Ph.D. dissertation, Mass. Inst. Tech., Cambridge (1962).

Manuscript received September 9, 1967; revision received April 26, 1968; paper accepted April 29, 1968. Paper presented at AIChE Tampa meeting.

Foaming and Frothing Related to System Physical Properties in a Small Perforated Plate Distillation Column

R. P. LOWRY and MATTHEW VAN WINKLE

The University of Texas, Austin, Texas

Experimental froth heights occurring on a perforated distillation tray were correlated with the determining system physical properties under distillation conditions. A photographic technique was used to measure accurately the foam and froth heights, produced in the 4 in. square test section of a laboratory distillation column, for several points in the composition range of five binary systems. Plate design parameters and operating vapor and liquid rates were held constant throughout the experimental study.

The froth height results from this investigation (*11*), as well as those from studies (*17*) of a 6 in. distillation column, show a linear relation with the expression, $U_A^2 \rho_V/(\rho_L - \rho_V)$, the frothing factor, for the ranges of the physical properties investigated.

The foam height results of this study indicate that the mass transfer surface tension gradient, the heat transfer gradient, and the absolute value of surface tension all contribute to foam formation and stability. Because of the complex relation between the surface tension gradient and the frothing factor in relation to the degree of foaming, as well as the effects of other influencing variables, a unique correlation of the foam height data resulting from mass transfer in this study was not feasible. However, it was possible to interpret quantitatively the nature of the effect for several of the data points.

This investigation was conducted to obtain experimental data which could provide a basis for correlation of the foam and froth heights occurring on an operating perforated distillation tray with system physical properties.

Depending on operating conditions and the system used, it is possible for either froth or foam to be formed on an operating distillation tray. Mukhlenov (*13*) and Pozin, et al. (*16*) describe froth as a vapor-liquid dispersion composed of small bubbles of vapor intermingled with streams of aerated liquid. Calderbank and Rennie (*4*) describe foam as comprised of large, cellular, relatively stable bubbles in close proximity.

The primary factor which determines whether froth or foam can be produced from a given liquid-vapor system is the ability of the liquid to form stable films as the vapor bubbles rise from the layer of liquid on a distillation tray into the space above. A system which exhibits this characteristic is generally referred to as a *foaming* system. A system which produces only froth on a distillation tray is usually called a *nonfoaming* system: Kitchener and Cooper (*8*) state that the property which distinguishes foaming from nonfoaming liquids is the ability to resist excessive localized thinning of a membrane (liquid film) while a controlled general thinning proceeds. This property is demonstrated in the effect of mass transfer on the surface tension of a film described by Zuiderweg and Harmens (*21*) and is characterized by the existence of surface tension gradients in the bubble laminae.

Vapor rate exerts an important influence on the nature of the vapor-liquid dispersion that actually occurs on a distillation tray. Several investigators (*2, 4, 12, 13, 15, 16, 18, 21*) have observed that low vapor rates favor the for-

---

R. P. Lowry is with the Celanese Chemical Company, Corpus Christi, Texas.

mation of foam (provided the liquid in question is capable of producing stable films). An increase in the vapor rate results in the mechanical destruction of this cellular foam and the simultaneous production of the clouds of smaller bubbles characteristic of froths. Pozin, et al. (*16*) estimated that cellular foam usually occurs at vapor velocities (based on the total cross section of flow path) less than 3.28 ft./sec. and that froth is the dominant type of two phase disperse system formed over a vapor velocity range of 2.3 ft./sec. to around 13 ft./sec. Significantly, Pozin and Tumarkina (*15*) note that at the higher vapor velocities both foaming and nonfoaming liquids show similar characteristics.

The vapor rate ranges cited are approximate since plate geometry, liquid rate, and particularly the magnitude of the surface tension gradients produced in the liquid influence the range of vapor rates at which the foam and froth regimes exist. Rennie and Evans (*18*) studied the effect of plate characteristics on foaming and frothing and observed that the formation of foam on a sieve tray is facilitated by closely spaced holes (resulting in large free areas), small diameter holes, and low liquid flow rates.

Some work has been devoted to correlating froth height data. Mukhlenov (*13*) and Pozin and Tumarkina (*15*) investigating nondistilling systems showed that froth height is an inverse function of surface tension and liquid viscosity and that within certain limits the vapor density does not influence froth height. These investigators gave no estimate of the precision of the froth height data and no indication of how the froth height measurements were obtained. By using froth height data obtained in a study (*1*) for a 2-ft. bubble-cap column for ammonia-air-water, acetone-benzene, and pentane-xylene systems, Hughmark (*7*) derived an empirical correlation for froth height as a function $U_G{}^2\,\rho_V/(\rho_L-\rho_V)$ [proposed by Souders and Brown (*20*)], the weir height, and the height of the crest over the weir as calculated by the modified Francis weir formula. The AIChE Bubble Tray Design Manual (*1*) included a correlation of froth height with vapor F factor, F_V, and weir height. The froth heights in the study (*1*) were obtained by visual observation, and the accuracy of the observations was estimated to be probably ± 0.5 in. The investigation described here studied foaming and frothing for actual distilling systems of widely varying physical properties, under conditions where the precision of the froth and foam height measurements was estimated to be ± 0.1 in.

EXPERIMENTAL PROCEDURE

A photographic technique was used to measure accurately the foam and froth heights that resulted from operation of a small perforated plate at distilling conditions. Several data points were obtained over a range of composition for each of five binary systems, which were selected to cover a reasonably broad range of system physical properties (specifically, vapor and liquid density, vapor and liquid viscosity, and surface tension). Plate design and the operating vapor and liquid rates were held constant throughout the experimental study to isolate system physical property effects. A vapor velocity leaving the test tray of 1.7 ft./sec. (based on the total cross-sectional area of the test section) and a liquid rate entering the test tray of 0.672 g./min./ft. of weir were selected to reflect typical plate operation, that is, no weeping or excessive entrainment. The binary systems used in the experimental study were acetone-butanol, methanol-1, 4-dioxane, carbon tetrachloride-propanol, propanol-water, and water-butanol. The use of these five binaries permitted the observation and study of both froth and foam formation.

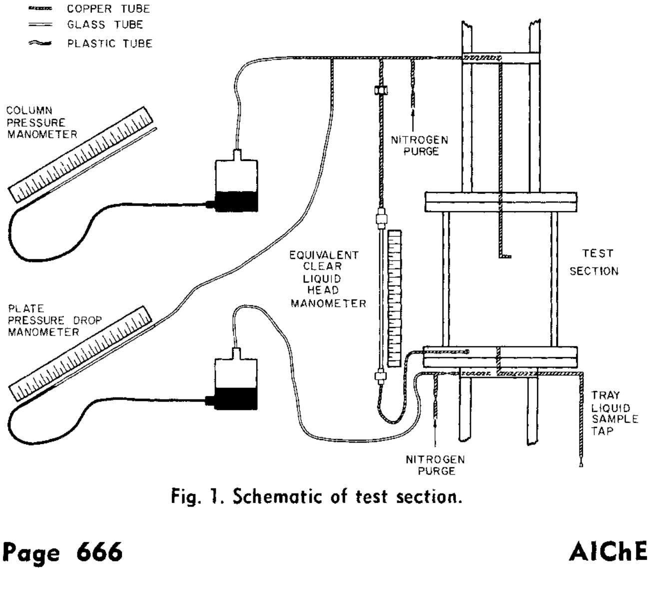

Fig. 1. Schematic of test section.

All organic chemicals used in this study were of reagent grade purity and laboratory distilled water was used in the two water-alcohol binaries (*11*). Data on the liquid density and the surface tension at the bubble point for the five binaries investigated were obtained from a study by Ling and Van Winkle (*9, 10*). Saturated vapor densities at the dew point were calculated for all five binaries by the method of Pitzer, et al. (*14*).

The experimental work was carried out in a glass laboratory distillation column consisting of a 4 in. square glass test section, 6¾ in. in height, with 3 in. I.D. aligning zones located above and below the test section. The use of the square test section minimized the optical distortion characteristic of a round glass section (*11*). Table 1 summarizes the important dimensions of the test section and the test plate. Figure 1 is a schematic of the test section and illustrates the pressure measurement arrangement for measuring the pressure drop across the operating test plate, the pressure in the test section, and the equivalent clear liquid head on the test plate.

TABLE 1. TEST SECTION SPECIFICATIONS

Cross-sectional area of square duct (sq. in.)	13.7
Height of square duct (in.)	6.75
Perforation diameter (in.)	0.125
Tray thickness (in.)	0.125
Pitch, on equilateral triangular centers (in.)	0.250
Numbers of perforations	90
Free area (% square test section cross-sectional area)	8.1
Downcomer area (% square test section cross-sectional area)	9.5
Active or bubbling area of tray (sq. in.)	5.14
Weir heigth (in.)	0.70
Weir length (in.)	3.22

Each data point was obtained for a predetermined set of conditions after operating the equipment under steady state conditions for 1 hr. Five photographs of the bubbling action in the test section were taken at 1 min. intervals (*11*) with a reflex camera at 1/500 sec. exposure. This procedure was repeated after a half-hour interval as a check on attainment of steady state conditions.

The average foam or froth height from the ten photographs, $\overline{H}_{F(10)}$, was used in the correlation work. An estimate of the precision of the data was made using data obtained on an air-water system. The estimate of the 90% confidence limits of $\overline{H}_{F(10)}$ can be expressed by Equation (1):

$$\overline{H}_{F(10)} - 0.098 < \mu < \overline{H}_{F(10)} + 0.098 \qquad (1)$$

Considering the violently fluctuating level that was being measured, such precision is considered highly satisfactory.

RESULTS

During the course of the experimental operation, both foam and froth were observed on the test tray. The photographs in Figure 2 clearly illustrate the nature of the foam and froth regimes observed in this study. The experimental data point associated with each photograph is indicated. In Figures 2*a* and 2*b* the cellular structure of the bubbles is a characteristic of foaming that has been noted by vir-

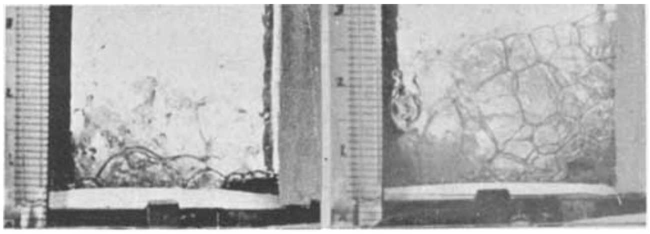

a. **M/D-5B (foam)**
$\overline{X}_T = 0.794$ mole fraction methanol
$\overline{H}_{F(10)} = 1.64$ in.

b. **P/W-25B (foam)**
$\overline{X}_T = 0.134$ mole fraction propanol
$\overline{H}_{F(10)} = 2.18$ in.

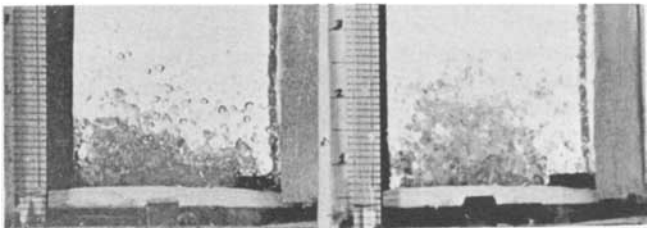

c. **M/D-17A (froth)**
$\overline{X}_T = 0.064$ mole fraction methanol
$\overline{H}_{F(10)} = 1.45$ in.

d. **C/P-1C (froth)**
$\overline{X}_T = 0.883$ mole fraction carbon tet.
$\overline{H}_{F(10)} = 1.94$ in.

Fig. 2. Illustrations of foam and froth.

tually all investigators who have studied the nature of foaming. Figure 2*c* and 2*d* indicate the existence of a very dense collection of finely dispersed liquid droplets above the test tray, and there is little evidence of the presence of bubbles of vapor. This description of froth is contrary to that suggested by other investigators, in which clouds of comparatively small bubbles were recognized as a characteristic of froth. The observations from this study indicate that a froth layer on an operating distillation tray is best described as a vapor-liquid dispersion characterized chiefly by the suspension of liquid in a stream of rising vapor.

DATA ACCURACY AND REPRODUCIBILITY

Precautions were taken in this investigation (*11*) to minimize the possibility of the presence of surface-active contaminants on the test tray and to analyze carefully the foam and froth height results, both qualitatively and quantitatively, for indications of the presence of such contaminants. From the results of this detailed analysis it was concluded that neither foam nor froth height measurements reflected the presence of contaminants in the test liquid.

ANALYSIS OF FROTH HEIGHT DATA

The lower set of data in Figure 3* is a plot of the average froth height [$\overline{H}_{F(10)}$] vs. the average frothing factor $(FF_C) = U_A^2\,\rho_V/(\rho_L - \rho_V)$ for the experimental froth height data obtained in this study. The average frothing factor is based on the average condition of the vapor entering and leaving the test tray. The lower line, a least squares fit shows a linear correlation of froth height with frothing factor. The deviations of the data points from the line are indicative of the precision of the ten-picture-average froth heights [$\overline{H}_{F(10)}$] used in the correlation and reflect the 90% confidence limits of the data, approximately ± 0.1 in. The least squares regression analysis shows an average absolute deviation of 2.9% and a maximum deviation of −11.7%. These results confirm that inertia (velocity — density) effects, reflected in the frothing factor, are the controlling influence in determining froth height. There is no indication that either surface tension or liquid viscosity are of significance within the range of properties studied in this investigation.

Since the vapor velocity was held approximately constant in this study, the range of the frothing factor over which the correlation applies reflects primarily a variation in vapor density (0.0006 to 0.00512 g./cc.) and liquid density (0.72 to 1.43 g./cc.). To confirm that vapor velocity quantitatively affects the froth height in the manner reflected by the frothing factor, Redwine's (*17*) froth height results obtained over a vapor velocity range of 1.05 to 3.32 ft./sec. and a vapor density range of 0.00208 to 0.00305 g./cc. were studied. The upper set of data in Figure 3 illustrates a plot of Redwine's average froth height data vs. frothing factor for the two systems studied, and a linear correlation with frothing factor also results with an average absolute deviation of 2.3% and a maximum deviation of 6.7%.

The lines for the two sets of data are virtually parallel but the line representing the data of this study predicts froth heights 0.25 in. less than the curve representing Redwine's data. This difference is considered to be the result of differences in the weir heights, 0.75 and 0.70 in. and liquid rates, from 0.59 to 3.02 and 0.672 g./min./ft. of weir used in the two studies. Redwine's data reflects a relatively wide range of liquid rates. Also, both parameters (liquid rate and weir height) influence the froth height on the tray.

ANALYSIS OF FOAM HEIGHT DATA

The foaming characteristics observed here are assumed to result from mass transfer surface tension gradients in the liquid films. Zuiderweg and Harmens (*21*) proposed the following mechanism for bubble film stability. As mass transfer occurs from the surfaces of liquid films enclosing bubbles of vapor, the thinner regions of the films become more quickly saturated in the less volatile component than the liquid bulk and the thicker liquid film regions, which

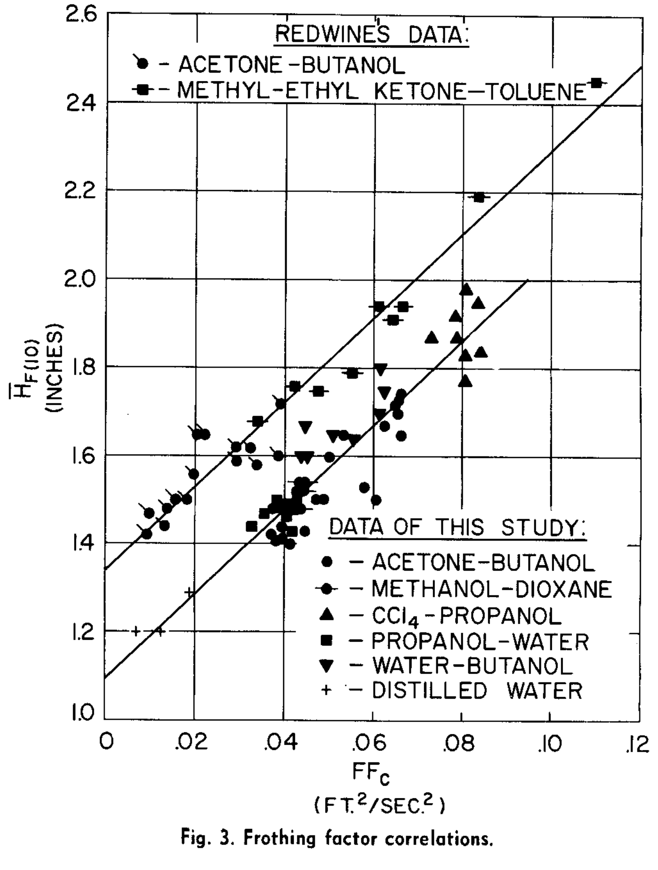

Fig. 3. Frothing factor correlations.

Tables 2 and 3 have been deposited as document NAPS-00484 with the ASIS National Auxiliary Publications Service, c/o CCM Information Sciences, Inc., 22 W. 34th St., New York 10001 and may be obtained for $1.00 for microfiche or $3.00 for photocopies.

occur at the junctions of the films. If the less volatile component has a higher surface tension, the thinner regions will experience an increase in surface tension and consequently will contract, drawing liquid from the liquid bulk and the thicker regions into the thinner areas. The thickness of the films *will be increased*, opposing the destructive effects of film expansion and drainage, and a net stabilization of the films results. If the less volatile component has a lower surface tension, liquid is drawn from the thinner regions of the films and rupture of the film takes place. On the basis of this mechanism a criterion for predicting the occurrence of foam on a distillation tray as a result of mass transfer is proposed. If a decrease in content of the more volatile component in the liquid films (caused by mass transfer) produces an increase in the surface tension, foam will appear on the tray; if a decrease in content of the more volatile component in the liquid films produces a decrease or no change in the surface tension, only froth will occur on the tray.

The experimental foam and froth height results for the methanol-dioxane and propanol-water binaries, in this study, confirm the foregoing criterion and serve as a possible basis for a quantitative measure of the effect. Consistent with the above postulate it follows that the magnitude of the mass transfer surface tension gradient, which is related to the rate of mass transfer from the films and the nature of the surface tension-composition relation, should exert a controlling influence on the degree of foaming that results from mass transfer. Equation (3) was derived (*11*) to express approximately the average mass transfer surface tension gradient ($\overline{\Delta\sigma}$) that exists between thin liquid bubble films and the liquid on an operating distillation tray with which the films are in contact at any time, θ, after the formation of the films:

$$\overline{\Delta\sigma} = \overline{\Delta\sigma}' \; [1 - \exp\,(-2K_x \; \theta/\rho_m t)] \tag{2}$$

$\overline{\Delta\sigma}'$ is defined as the average potential mass transfer surface tension gradient, which is simply the surface tension gradient that would be established if the films of liquid were in equilibrium with the vapor phase, with which they are in contact on the tray. (From the definition of $\overline{\Delta\sigma}$ and $\overline{\Delta\sigma}'$, foaming will occur only in the case of positive values of these variables.)

In Equation (2), $\overline{\Delta\sigma}'$ can be regarded as the principal driving force in establishing the surface tension gradient between the films of liquid and liquid on the tray. It reflects the combined influence of the liquid phase driving force and the slope of the surface tension-composition curve [the results of Zuiderweg and Harmens (*21*) also indicate that both of these parameters influence the degree of foaming resulting from mass transfer]. $\overline{\Delta\sigma}'$ can be determined from the average liquid composition on the tray and the average vapor composition above the tray. The surface tension of the liquid mixture of average composition on the tray is subtracted from the surface tension, corresponding to the liquid composition in equilibrium, with the average vapor composition above the tray to obtain $\overline{\Delta\sigma}'$.

The average mass transfer surface tension gradient ($\overline{\Delta\sigma}$) in Equation (2) is also a function of the expression $[1 - \exp(-2K_x\theta/\rho_m t)]$. This term is characteristic of a dynamic first-order step response and varies from zero to unity as θ increases from zero to infinity. In effect this expression determines the fraction of the average potential mass transfer surface tension gradient that actually exists at any time, θ, after the formation of the liquid films. In addition to θ, the magnitude of this term is also determined by the overall liquid phase mass transfer coefficient, K_x, the thickness of the films, t, and the liquid molal density, ρ_m.

Inability to predict the value of the term $[1 - \exp\,(-2K_x\theta/\rho_m t)]$ complicates quantitative analysis of the effect of mass transfer on the degree of foaming. The determination of the film thickness, t, in relation to the operating conditions and physical properties of the system presents a potentially formidable problem. It is also difficult to predict accurately the lifetime of bubble films on an operating tray (in relation to their destruction by the vapor stream), which should set an upper limit on the value of θ. With regard to the apparent relationship between θ and the lifetime of the bubble films, it appears that the frothing factor should exert a related effect on the degree of foaming resulting from mass transfer (because of its destructive effect on bubble films). Other factors which can have an influence on the degree of foaming are surface elasticity (3), heat transfer, and the magnitude of equilibrium surface tension. It was concluded that the surface elasticity effect was of minor importance in the analysis of the foam height data resulting from mass transfer in this investigation. It has been observed (5) that under distillation conditions heat transfer from the gas to the liquid can produce surface tension gradients opposite in direction to the mass transfer gradient, thus retarding the effect of mass transfer. Consequently, the opposing effect of temperature gradients are of importance in the analysis of the effect of mass transfer surface tension gradients on the degree of foaming. The effect of the magnitude of the equilibrium surface tension, from a purely energetic standpoint, on the large increase in interfacial area that occurs in the formation of the bubble films in foam also could be of importance in this analysis.

Because of the complex relationship between the mass transfer surface tension gradient and the frothing factor related to the degree of foaming that results from mass transfer and the possible influence of heat transfer and the influence of the level of the equilibrium surface tension, a unique correlation of the foam height data resulting from mass transfer in this study was not feasible. However, it was possible to interpret quantitatively the nature of the effect for several of the data points for which it was observed. Figures 4 and 5 respectively illustrate those data points for the propanol-water binary and the methanol-dioxane binary for which such an analysis was possible. In these two graphs the foam ratio is plotted vs. $\overline{\Delta\sigma}'$. The foam ratio is defined as the ratio of the measured foam height to the height predicted by the frothing factor correlation (Figure 3) and is simply a measure of the degree of foaming. Since $\overline{\Delta\sigma}$ can not be determined, because of the inability to evaluate the term $[1 - \exp(-2K_x\theta/\rho_m t)]$, $\overline{\Delta\sigma}'$ is used in Figures 4 and 5 to relate indirectly the effect of $\overline{\Delta\sigma}$ on the degree of foaming. This substitution is valid provided the term $[(1 - \exp(-2K_x\theta/\rho_m t)]$ remains constant over the range of the data analyzed. Further, in the relations shown in Figures 4 and 5 the possible coincident effects of frothing factor, temperature gradients, and the equilibrium surface tension must be accounted for if the analysis is to have any meaning.

For the propanol-water data plotted in Figure 4 the frothing factor covers a range of 0.0246 to 0.0280 sq.ft./sec.^{2} and for the methanol-dioxane data, Figure 5, a range of 0.0368 to 0.0401 sq.ft./sec.^{2}. The propanol-water data correspond to an average tray liquid composition of 0.136 to 0.281 mole fraction propanol, and the methanol-dioxane data an average composition of 0.737 to 0.913 mole fraction methanol. Consequently, for each set of data plotted in Figures 4 and 5, the related effect of frothing factor should be constant and the term $[1 - \exp(-2K_x\theta/\rho_m t)]$ also should be constant. [It also is noted that surface tension varies over a small range for the data plotted in Figures 4 and 5 (18.9 to 22.8 dynes/cm.), and for both sets of data the temperature gradient across the test tray is small (less than 4°F.).] Therefore, the possible related effects of these two variables should not affect the nature of the plots appreciably.

For the propanol-water data in Figure 4 the increase in the foam ratio with an increase in $\overline{\Delta\sigma}$, for the range of $\overline{\Delta\sigma}'$ for these data points, is quite clear. A dashed line has been drawn to indicate the suggested trend of the data. In light of the mechanism postulated for the occurrence of foam under conditions of mass transfer, this trend seems reasonable. Hence, these results illustrate the usefulness of Equation (2) in predicting the degree of foaming resulting from mass transfer. In Figure 5 the methanol-dioxane data indicate an increase in foam ratio with an increase in $\overline{\Delta\sigma}'$ but because of the low foam ratios the precision of the foam height measurements tends to limit their significance.

CONCLUSIONS

The nature of froth as described in this study indicates that inertia effects and not surface effects are controlling in predicting froth height. The experimental froth height data of this study, which correspond to a broad range of vapor and liquid density, vapor and liquid viscosity, and surface tension, show a linear relation with the expression, $U_A{}^2\,\rho_V/(\rho_L - \rho_V)$. For the plate geometry and liquid rate used in this investigation, the froth height can be predicted accurately [2.9% average absolute deviation by Equation (3)]:

$$\overline{H}_F = 1.09 + 9.65\,\frac{U_A{}^2\,\rho_V}{\rho_L - \rho_V} \qquad (3)$$

The experimental froth height results obtained by Redwine (*20*) correlate similarly with the frothing factor, as shown by Equation (4), with 2.3% average absolute deviation.

$$\overline{H}_F = 1.34 + 9.52\,\frac{U_A{}^2\,\rho_V}{\rho_L - \rho_V} \qquad (4)$$

Further study is required to determine the effects of plate geometry and liquid rate, which are assumed to account for the difference in the intercepts of Equations (3) and (4).

The foam height results of this study tend to confirm that the average mass transfer surface tension gradient, ($\overline{\Delta\sigma}$), established between liquid films and the liquid on the tray, defined by Equation (2), exerts a controlling influence on the degree of foaming that results from mass transfer.

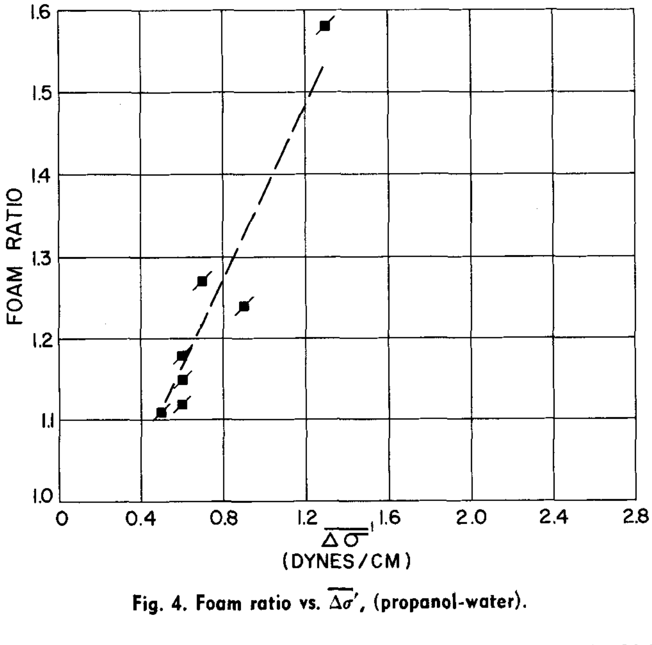

Fig. 4. Foam ratio vs. $\overline{\Delta\sigma}'$, (propanol-water).

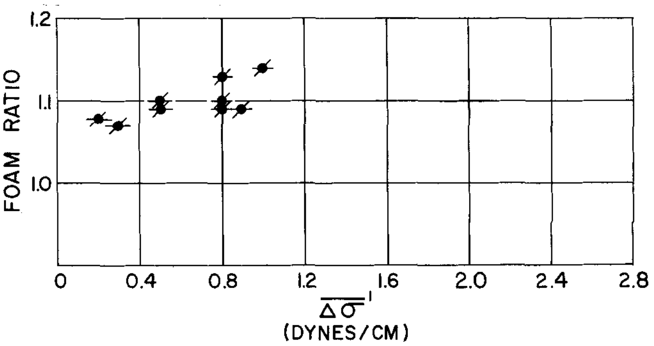

Fig. 5. Foam ratio vs. $\overline{\Delta\sigma}'$, (methanol-dioxane).

Mass transfer surface tension gradients are most pronounced in binary systems for which the surface tension-composition curve exhibits a relatively large slope [the occurrence of foam will depend on the sign of the derivative ($\overline{d\sigma/dx}$) in relation to the foaming criterion stated earlier]. Further, the existence of large liquid phase driving forces increases the degree of foaming that results from the effect as shown in Figure 4.

The foaming effect is more pronounced at low frothing factors because the increased momentum of the vapor at higher values destroys the stable foam bubble films. Foaming is the result of a complicated interaction of the mass transfer surface tension gradients with frothing factor, temperature gradients, and the level of the equilibrium surface tension, which at the present cannot be explained in a satisfactory quantitative form.

ACKNOWLEDGMENT

The authors wish to acknowledge gratefully the support of the National Science Foundation, whose grant sponsored this research, and the National Aeronautics and Space Administration and the Engineering Foundation, whose fellowship programs financially supported one of the authors.

NOTATION

F_V = $U_A\sqrt{\rho_V}$ = F-factor (ft./sec.) (lb./cu.ft.)$^{1/2}$

FF_C = $U_A{}^2\rho_V/(\rho_L - \rho_V)$ = average frothing factor; average for the condition of the vapor entering and leaving the tray; the vapor rates have been corrected to allow for condensation due to heat transfer, sq.ft./sq.sec.

$\overline{H}_F$ = average foam (or froth) height, in.

$\overline{H}_{F(10)}$ = average foam (or froth) height, in.

K_x = overall mass transfer coefficient, g.-moles/sec. sq.cm., (mole fraction)

t = film thickness, cm.

U_A = vapor velocity based on active (or bubbling) area in the test section, ft./sec.

U_G = vapor velocity based on the active (or bubbling) area of the tray, ft./sec.

$\overline{X}$ = liquid composition (mole fraction light component)

Greek Letters

$\overline{\Delta\sigma}$ = average mass transfer surface tension gradient, dynes/cm.

$\overline{\Delta\sigma}'$ = average potential mass transfer surface tension gradient, dynes/cm.

θ = time, sec.

μ = true value of foam (or froth) height, in.

ρ_L = liquid density, g./cc.
ρ_M = liquid molal density, g.-moles/cc.
ρ_V = vapor density, g./cc.
σ = surface tension, dynes/cm.

LITERATURE CITED

1. American Institute of Chemical Engineers, *AIChE Bubble Tray Design Manual*, New York (1958).
2. Aksel'rod, L. S., et al., *J. Appl. Chem. U.S.S.R.*, **29**, 1939 (1956).
3. Andrew, S. P. S., *Proc. Intern. Symp. Dist., England*, 73 (1960).
4. Calderbank, P. H., and J. Rennie, *Trans. Inst. Chem. Engr.*, **40**, 3(1962).
5. Danckwerts, G. C., H. Sawistowski, and W. Smith, *Proc. Intern. Symp. Dist., London*, 9 (May, 1960).
6. Gibbs, J. W., *Collected Works*, **1**, Longmans Green, pp. 300-314 (1928).
7. Hughmark, G. A., *Chem. Engr. Prog.*, **61**, 97 (July, 1965).
8. Kitchener, J. A., and C. F. Cooper, *Quart. Rev. (London)*, **13**, 71 (1959).
9. Ling, T. D., and M. Van Winkle, *J. Chem. Eng. Data*, **3**, 82 (1958).
10. *Ibid.*, 88 (1958).
11. Lowry, R. P., Ph.D. dissertation, Univ. Texas (1967).
12. Mukhlenov, I. P., *J. Applied Chem. U.S.S.R.*, **30**, No. 3, 1819 (1958).
13. ———, *Zhur. Priklad. Khim.*, **31**, No. 1, 45 (1958).
14. Pitzer, K. S., et al., *J. Am. Chem. Soc.*, **77**, 3427 (1955).
15. Pozin, M. E., and E. S. Tumarkina, *J. Applied Chem. U.S.S.R.*, **27**, 1109 (1954).
16. ———, I. P. Mukhlenov, and E. Ya. Tarat, *Zhur. Priklad. Khim.*, **30**, No. 1, 45 (1957).
17. Redwine, D. A., M. thesis, Univ. Texas (1967).
18. Rennie, J., and F. Evans, *Brit. Chem. Eng.*, **7**, 498 (1962).
19. Robinson, J. V., et al., *J. Phys. Colloid Chem.*, **52**, 763 (1948).
20. Souders, Mott, Jr., and G. G. Brown, *Ind. Eng. Chem.*, **26**, 98 (Jan., 1934).
21. Zuiderweg, F. J., and A. Harmens, *Chem. Eng. Science*, **9**, 89 (1958).

Manuscript received July 29, 1967; revision received May 22, 1968; paper accepted May 24, 1968.

An Experimental Study of Steady State Multiplicity in a Loop Reactor

R. B. ROOT and R. A. SCHMITZ
University of Illinois, Urbana, Illinois

Steady state multiplicity in an adiabatic loop reactor was studied in experiments employing the reaction between sodium thiosulfate and hydrogen peroxide in aqueous solution. The steady state characteristics of the loop reactor were predicted by a method which utilized batch reactor data of temperature vs. time directly. The method was based on the assumption of plug flow with negligible axial dispersion and on a single-step chemical kinetic model. Experimental results verify the existence of multiple steady states on ranges of feed flow rates and recycle ratios and demonstrate the capability of the simple model for predicting the qualitative and quantitative features of the reactor steady state.

Some observations were made of the effect of large disturbances on the stability of the reactor while operating in a multiple state region. Results for such cases illustrate reactor instability in the sense that a transition to a new steady state takes place provided the disturbance is sufficiently large.

The distinctive features of steady state multiplicity and instability in continuous flow exothermic processes were first introduced to the field of chemical reactor design in a publication by Van Heerden in 1953 (*1*). Bilous and Amundson (*2*), and Aris and Amundson (*3*) examined these features for a perfectly mixed reactor on a firm mathematical basis, and subsequent theoretical studies have been numerous. At the present time a wealth of theory is available regarding steady state characteristics, stability, and control of various lumped and distributed parameter models of exothermic reaction systems. However, with the exception of a recent study by Padberg and Wicke (*4*) of a catalytic reaction in a fixed-bed reactor, experimental data or reports in the literature of actual experiences relative to steady state multiplicity and stability in chemical reactors are lacking.

This paper presents the results of an experimental study which involved a laboratory tubular reactor with recycle, referred to hereafter as a *loop* reactor, and employed the reaction between sodium thiosulfate and hydrogen peroxide in aqueous solution. The study was undertaken to obtain experimental observations and data regarding steady state multiplicity and stability and to test the capability of a simple model for describing these characteristics. Presented herein are the results of the first phase of the work which focuses on stable steady states in the multiple state regime of an adiabatic system.

The loop reactor was chosen for experimentation for two principal reasons: 1. theoretical background is available for guidance (*5* to *8*), and 2. this type of reactor provides the advantage, as will be shown later, that steady state characteristics for an adiabatic plug flow model may be predicted directly from batch reactor data of temperature vs. time without requiring a kinetic expression. Furthermore, recycle processes are of importance industrially.

Since reaction kinetic expressions are seldom sufficiently accurate to permit a complete exploration of parameters and conditions, it is a significant advantage in studies of the loop reactor that performance characteristics may be predicted directly from batch reactor data of temperature vs. time. Such data are relatively easy to obtain in a liquid system. It is possibly the lack of sufficient kinetic data or the difficulty in obtaining sufficient data that has heretofore discouraged researchers from undertaking experimental studies of nonisothermal reactors and has channeled most efforts toward theoretical work and computer simulations employing hypothetical reactions.

R. B. Root is with E. I. du Pont de Nemours and Company, Wilmington, Delaware.